DETC2000/PTG-14432

DYNAMICS OF HYPOID GEAR TRANSMISSION WITH NON-LINEAR TIME-VARYING MESH

Yuping Cheng
Department of Mechanical Engineering, The Ohio State University, 206 West 18th Avenue, Columbus, OH 43210, USA

Teik C. Lim
Department of Mechanical Engineering, 290 Hardaway Hall, Box 870276, University of Alabama Tuscaloosa, AL 35487, USA

ABSTRACT

A new generalized 14 degrees-of-freedom dynamic model with coupled translation-rotation effect is developed for simulating the non-linear vibratory response of hypoid geared rotor systems. The model incorporates the load-dependant time-varying mesh characteristic vectors due to tooth load sharing and profile modifications, backlash non-linearity, and off line-of-action friction forces. Based on the 3-dimensional tooth contact analysis results, the quasi-static mesh characteristics that describe the translation-rotation and rotation-rotation force couplings are obtained for use in the dynamic formulation. The three-dimensional representations of the mesh vectors, normal and friction forces, and moments generated at the mesh interface are also included in the proposed study. Tooth separation and the occurrence of jump phenomenon observed in the predicted frequency response functions are analyzed.

INTRODUCTION

It is generally known that the gear kinematic transmission error is the primary source of vibratory energy excitation that produces tonal noise in most geared applications. Extensive efforts have been made to synthesize of machine tool and cutter settings to manufacture desired hypoid gear tooth profiles and contact patterns (Fong and Tsay, 1991, 1992; Gosselin et. al., 1989; Litvin et. al., 1981, 1989, 1991, 1998; Kubo et. al., 1997). However, very few research has been performed to study the system dynamic aspects of non-parallel gearing. From the open gear literature, one can only find a few analytical studies (Remmers, 1971; Pitts, 1972; Kiyono et. al., 1981; Nakayashiki, et. al., 1983; Abe and Hagiwara, 1990) on hypoid gear vibrations, even though the dynamics of parallel axis gears have been investigated extensively as reported in typical References (Özgüven and Houser, 1988; Kahraman and Singh, 1990; Blankenship and Singh, 1995; Velex and Maatar, 1996). Of the few studies that exist on hypoid gear dynamics, many actually ignored the excitation of transmission error (TE). A recent model suggested by Donley et al. (1992) was based on an approximate hypoid gear mesh formulation for use in the context of a linear time-invariant dynamic finite element representation, which relies on a bevel gear mesh equivalence theory. Also, none of the above hypoid gear dynamics studies clearly define the mesh coupling precisely, and the theoretical models essentially rely on simplified mesh force vector representation. More recently, Lim and Cheng (1998, 1999) proposed a new mesh coupling formulation for spiral bevel and hypoid gears, and studied the dynamic response applying a linear time-invariant model.

The present study presents a time-varying 3-dimensional mesh coupling characteristics of hypoid gears, and includes the effects of friction and backlash type non-linearity as well as time-dependent mesh position and line-of-action vectors. The proposed spatial and load dependent mesh stiffness and transmission errors are then incorporated into a multi-degrees-of-freedom dynamic model of the hypoid geared rotor system. Numerical simulation results applying this non-linear time-varying mesh model are examined to gain a better understanding of the vibratory response of this class of gears.

GEAR MESH MODEL

A 3-dimensional tooth contact analysis is performed using the Contact Analysis Program Package (CAPP) that is based on the finite element and surface integral methods (Vijayakar, 1987, 1991). The code employs a Simplex type algorithm to simulate the elastic gear tooth contact problem. The time-varying mesh position/stiffness, line-of-action, loaded transmission error, and normal and friction load distributions are computed from the simulation. In this approach, the contact areas of the gear teeth are discretized into a series of smaller cells. Each cell contains a localized compliance c_{ij} that is a function of the spatial dimensions, gear mesh position and applied mean torque. The position vector of each contact cell i in the coordinate system S_l represented by X_l, Y_l and Z_l axes, l = 1 (pinion) or 2 (gear), is $\boldsymbol{r}_i^{(l)} = \{x_i^{(l)}\ y_i^{(l)}\ z_i^{(l)}\}^T$, while the unit normal vector is given by $\boldsymbol{n}_i^{(l)} = \{n_{ix}^{(l)}, n_{iy}^{(l)}, n_{iz}^{(l)}\}^T$ as shown in Figure 1. The projection of the unit normal vector into the tangential direction of rotational motion relative to S_l can be expressed as

$$l_{ix}^{(l)} = \boldsymbol{n}_i^{(l)} \times (\boldsymbol{i}^{(l)} \cdot \boldsymbol{r}_i^{(l)}) \; ; \; l_{iy}^{(l)} = \boldsymbol{n}_i^{(l)} \times (\boldsymbol{j}^{(l)} \cdot \boldsymbol{r}_i^{(l)}) \; ;$$
$$l_{iz}^{(l)} = \boldsymbol{n}_i^{(l)} \times (\boldsymbol{k}^{(l)} \cdot \boldsymbol{r}_i^{(l)}) \qquad (1)$$

where $\boldsymbol{i}^{(l)}$, $\boldsymbol{j}^{(l)}$ and $\boldsymbol{k}^{(l)}$ are the triad of unit vectors that defines the axes of S_l. Hence, the directional cosine of each cell i clearly depends on the gear geometry and its actual mesh position. Here, the dimensional mesh parameter $l_{iu}^{(l)}$ $(u=x,y,z)$ is referred to as the directional rotation radius about the u-axis, which represents the tangential force component at the contact point i per unit normal force along $n_i^{(l)}$.

The relative sliding velocity vector with respect to S_0, where $S_o=S_2$, may be transformed into the local coordinate system S_l by $\{\boldsymbol{v}_i^{(l)}\} = [M_{l0}] \times \{\boldsymbol{v}_i^{(12)}\} = \{v_{ix}^{(l)}, v_{iy}^{(l)}, v_{iz}^{(l)}\}^T$. Projection of the relative sliding velocity vector in the tangential direction of rotational motion relative to X_l, Y_l and Z_l can be shown to be

$$t_{ix}^{(l)} = v_{iz}^{(l)} y_i^{(l)} - v_{iy}^{(l)} z_i^{(l)} \; ; \quad t_{iy}^{(l)} = v_{ix}^{(l)} z_i^{(l)} - v_{ix}^{(l)} x_i^{(l)} \; ;$$
$$t_{iy}^{(l)} = v_{ix}^{(l)} z_i^{(l)} - v_{ix}^{(l)} x_i^{(l)} \qquad (2)$$

Here $t_{iu}^{(l)}$ can be regarded as the tangential friction force component at contact point i per unit friction force in the sliding direction $v_i^{(l)}$.

The loaded transmission error (LTE) is resulted from the tooth errors and deflections due to base rotation, bending, shearing, and contact deformation. Assuming that the pinion and gear rotate about their respective Y-axes, their contact regions can be divided into N_c cells as shown in Figure 1. Here N_c is dependent on load and angular position. Since the rotations of all the simultaneously contacting cells are the same under load because of load sharing compatibility (Krenzer, 1986; Gosselin et al., 1995; Tavakoli and Houser, 1986, Vijayakar, 1987), the following expression for the equilibrium state of gear relative rotation (also known as the LTE of the pinion assuming fixed gear) can be derived as shown

$$\Delta q_L = \frac{M_1 - (\{\boldsymbol{?}_1\} - m\{\boldsymbol{T}_1\})[C_d]^{-1}\{\boldsymbol{E}_0\}^T}{(\{\boldsymbol{?}_1\} - m\{\boldsymbol{T}_1\})[C_d]^{-1}\{\boldsymbol{?}_1\}^T} \qquad (3)$$

where M_1 is the torque applied on the pinion, m is friction coefficient, $\boldsymbol{?}_1 = \{l_{1y}^{(1)} \; l_{2y}^{(1)} \ldots l_{N_c y}^{(1)}\}$ is a column vector of dimension N_c, which represents the increase in separation between the mating gear teeth at each individual cell position due to the angular displacement Δq_L, and $\{\boldsymbol{T}_l\} = \{t_{1y}^{(l)}, t_{2y}^{(l)}, \ldots, t_{Ncy}^{(l)}\}$. The compliance matrix $[C_d]$ represents the net compliance due to normal and friction loads acting on all cells. Note that the initial gear tooth separation is given by $\boldsymbol{E}_0^T = \{e_{01} \ldots e_{0N_c}\}^T$. Due to the deflection of the gear teeth and effect of load sharing, the tooth contacts are generally perturbed from their theoretical position.

DYNAMIC FORMULATION

Consider a generic driveline system comprising of a hypoid gear pair, an engine inertia, and a load element as shown in Figure 2. Each gear is modeled as a rigid conical body attached to a torsionally flexible shaft, which is supported by a compliant rolling element bearing represented by a set of discrete stiffness and damping elements (Lim and Singh, 1990). Recall that the nominal rotations of the pinion and gear are about Y_1 and Y_2 respectively. Furthermore, only the torsional coordinates of the engine and load are modeled as their translation coordinates that are normally decoupled from those of the gears by design. The mesh vectors, such as contact position and force vectors, under the dynamic condition are assumed to be the same as those for the static condition. In other words, the normal and friction load distributions, and line of action are assumed unperturbed by the vibratory response. This approach has also been used in previous studies on parallel gear dynamics (Kahraman and Singh, 1990; Özgüven and Houser, 1988(b); Blankenship and Singh 1995).

In order to improve computational efficiency and simplify the modeling process, the equivalent forces and moments will be used in the subsequent dynamic response simulation. Thus the above equations are used to seek the equivalent mesh characteristics as a function of angular position. To do so, consider the resultant normal force $F_{du}^{(l)}$ and friction force $F_{fu}^{(l)}$ along the u-axis where $u=x,y,z$:

$$F_{du}^{(l)} = \sum_{i}^{Nc} \sum_{j}^{Nc} n_{iu}^{(l)} k_{ij} d_j = \boldsymbol{N}_u^{(l)} [C_d]^{-1} \boldsymbol{?}_d = n_u^{(l)} W_0$$
$$F_{fu}^{(l)} = \sum_{i}^{Nc} \sum_{j}^{Nc} m v_{iu}^{(l)} k_{ij} d_j = m \boldsymbol{V}_u^{(l)} [C_d]^{-1} \boldsymbol{?}_d = m v_u^{(l)} W_0 \qquad (4)$$

where d_j is the deformation of cell j, $\boldsymbol{?}_d = \{d_1 d_2 \ldots d_{N_c}\}^T$, $\boldsymbol{N}_u^{(l)} = \{n_{1u}^{(l)} n_{2u}^{(l)} \ldots n_{N_c u}^{(l)}\}^T$, $\boldsymbol{V}_u^{(l)} = \{v_{1u}^{(l)} v_{2u}^{(l)} \ldots v_{N_c u}^{(l)}\}^T$, $[C_d]^{-1}\boldsymbol{?}_d$ is the normal force acting on the gear mesh interface, and W_0 is the equivalent static normal load acting on the meshing teeth which depends on the instantaneous transmission ratio. Equation (4) gives the averaged normal and friction forces by summing the loads associated with each individual cell. Thus, $n_u^{(l)}$ and $v_u^{(l)}$ are the equivalent normal and frictional force vectors. Similarly, the resultant moments contributed by the normal and friction forces about the u-axis are

$$M_{du}^{(l)} = \sum_{i}^{Nc} \sum_{j}^{Nc} l_i^{(l)} k_{ij} d_j = \boldsymbol{?}_u^{(l)} [C_d]^{-1} \boldsymbol{?}_d = l_u^{(l)} W_0$$
$$M_{fu}^{(l)} = \sum_{i}^{Nc} \sum_{j}^{Nc} m t_i^{(l)} k_{ij} d_j = m \boldsymbol{T}_u^{(l)} [C_d]^{-1} \boldsymbol{?}_d = m t_u^{(l)} W_0 \qquad (5)$$

where $\boldsymbol{?}_u^{(l)} = \{l_{1u}^{(l)} \; l_{2u}^{(l)} \ldots l_{N_c u}^{(l)}\}^T$ and $\boldsymbol{T}_u^{(l)} = \{t_{1u}^{(l)} t_{2u}^{(l)} \ldots t_{N_c u}^{(l)}\}^T$. The parameters $l_u^{(l)}$ and $t_u^{(l)}$ are the equivalent directional rotation radius of the normal and friction forces, respectively. The equivalent static normal load W_0 depends on time and is also a function of the pinion angular rotation position given by $W_0 = M_1 / (l_y^{(1)} - m t_y^{(1)})$.

Next, consider the pinion and gear member with 6 degrees-of-freedom (DOF) coordinates per member. Each coordinate is given by $\boldsymbol{q}_l(t) = \{x_l \quad y_l \quad z_l \quad q_{xl} \quad q_{yl} \quad q_{zl}\}^T$, where x_l, y_l and z_l are the translation coordinates, and q_{xl}, q_{yl} and q_{zl} are the angular coordinates. Since the mesh and friction forces are obtained under the quasi-static condition, the dynamic force and moment expressions can be further simplified by using the equivalent mesh vectors derived above. The

equivalent normal and friction forces acting on gear member l are given by

$$F_{du}^{(l)} = \sum_{i}^{Nc}\sum_{j}^{Nc} n_{iu}^{(l)} k_{ij} d_j = n_u^{(l)} k_m (\boldsymbol{h}^{(1)} \boldsymbol{q}_2 - \boldsymbol{h}^{(2)} \boldsymbol{q}_1 + e_0)$$
$$F_{fu}^{(l)} = \sum_{i}^{Nc}\sum_{j}^{Nc} m v_{iu}^{(l)} k_{ij} d_j = m v_u^{(l)} k_m (\boldsymbol{h}^{(1)} \boldsymbol{q}_2 - \boldsymbol{h}^{(2)} \boldsymbol{q}_1 + e_0) \quad (6)$$

respectively, where e_0 is the translation form of the unloaded kinematic transmission error in the direction of the line-of-action. The equivalent dynamic moments due to normal and friction forces are then given by

$$M_{du}^{(l)} = \sum_{i}^{Nc}\sum_{j}^{Nc} l_{iu}^{(l)} k_{ij} d_j = l_u^{(l)} k_m (\boldsymbol{h}^{(1)} \boldsymbol{q}_2 - \boldsymbol{h}^{(2)} \boldsymbol{q}_1 + e_0)$$
$$M_{uf}^{(1)} = \sum_{i}^{Nc}\sum_{j}^{Nc} m t_{iu}^{(l)} k_{ij} d_j = m t_u^{(1)} k_m (\boldsymbol{h}^{(1)} \boldsymbol{q}_2 - \boldsymbol{h}^{(2)} \boldsymbol{q}_1 + e_0) \quad (7)$$

respectively. Vector $\boldsymbol{h}^{(l)}$ denotes the mesh vector for a specific mesh position and applied pinion torque, and is given by $\boldsymbol{h}^{(l)}(t) = \{n_x^{(l)}\ n_y^{(l)}\ n_z^{(l)}\ l_x^{(l)}\ l_y^{(l)}\ l_z^{(l)}\}$. It can be noted that $\boldsymbol{h}^{(l)}$ is time-varying and load-dependent. The instantaneous $k_m(t)$ is a function of load, tooth errors, tooth modifications and gear rotation position. Accordingly, the equations of motion (14 DOF) incorporating loaded transmission error e_L are given by

$$I_E \ddot{q}_E + k_{t_1}(q_E - q_1) + c_{t_1}(\dot{q}_E - \dot{q}_1) = -T_1$$
$$[M_1]\{\ddot{q}_1\} + (\boldsymbol{h}^{(1)T} - m\boldsymbol{g}^{(1)T}) f(d_d - e_L) +$$
$$[C_{1b}]\{\dot{q}_1\} + [K_{1b}]\{q_1\} = \{F_{ext}^{(1)}\}$$
$$[M_2]\{\ddot{q}_2\} - (\boldsymbol{h}^{(2)T} + m\boldsymbol{g}^{(2)T}) f(d_d - e_L) +$$
$$[C_{2b}]\{\dot{q}_2\} + [K_{2b}]\{q_2\} = \{F_{ext}^{(2)}\}$$
$$I_O \ddot{q}_O + k_{t_2}(q_O - q_2) + c_{t_2}(\dot{q}_O - \dot{q}_2) = -T_2 \quad (8)$$

where, I_E and I_O are the mass moment of inertias of the driver and load, k_{t_1} and k_{t_2} are the torsional stiffnesses of the input and output shafts; c_{t_1} and c_{t_2} are the input and output shaft damping coefficients; T_1 and T_2 are the mean torques applied to the driver and load; $[M_l]$, $[K_{lb}]$ and $[C_{lb}]$ are mass matrix, equivalent stiffness and damping matrices of shaft-bearing components respectively, which will be given later; and $\{F_{ext}^{(l)}\}$ is the external load acting on the gear member l. The dynamic transmission error (DTE), denoted by d_d, is given by $d_d = \boldsymbol{h}^{(1)}\{\boldsymbol{q}_1\} - \boldsymbol{h}^{(2)}\{\boldsymbol{q}_2\}$. The time-varying and load-dependent vector for friction force is $\boldsymbol{g}^{(l)}(t) = \{v_x^{(l)}\ v_y^{(l)}\ v_z^{(l)}\ t_x^{(l)}\ t_y^{(l)}\ t_z^{(l)}\}$. In equation (8), the non-linear function $f(d_d - e_L)$ describes the elastic dynamic force that depends upon the operational condition, and can be defined as

$$f(d_d - e_L) = \begin{cases} W_0 + k_m(t)(d_d - e_L) + c_m(\dot{d}_d - \dot{e}_L) & \text{if } W_d > 0 \\ 0 & \text{if } W_d = 0,\ -b_c < d_d < 0 \\ W_0 + k_m(t)(d_d - e_L + b_c) + c_m(\dot{d}_d - \dot{e}_L + \dot{b}_c) & \text{if } W_d < 0,\ d_d < -b_c \end{cases} \quad (9)$$

$$W_d = W_0 + k_m(d_d - e_L) + c_m(\dot{d}_d - \dot{e}_L) \quad (10)$$

CASE STUDY

Now consider a reduced order model that includes the pinion and gear rotation and translation coordinates, torsional compliances of the shafts, and shaft-bearing stiffness. Also, the pitch and yaw motions of the gears are neglected. Hence, the total DOF of the system is 10 rather than 14. Since the system is semi-definite due to the rigid body rotational mode, we can transform the formulation into a positive-definite system by letting $u_1(t) = q_1 - q_E$; $u_2(t) = l_y^{(2)} q_2 - l_y^{(1)} q_1$; $u_3(t) = q_2 - q_O$. The above non-linear time-varying vibration equations can be integrated numerically using the 5/6th order Runge-Kutta integration routine with adaptive size. The result provides the time domain steady-state response. As part of the solution scheme, the second order differential equations must be casted in the state-space form generally given by $\dot{u}_i = f_i(u_1, u_2, ..., u_{18})$, where i=1,2,…,18. Note that the LTE calculated from CAPP is used as the input to this simulation. For a specific mesh position, the dynamic load can be computed from equation (10). Negative dynamic load indicates tooth separation. When this happens, the backside collision is then checked using equation (9).

A typical automotive hypoid gear set given in Table 1 is considered. First, the LTE and k_m are computed for different loading conditions. The present study found that the torque applied on the pinion significantly modifies the shape of the loaded transmission error, as shown in Figure 3(a). In the unloaded case, the TE is parabolic in shape and the gear lags the pinion. With increasing torque, the LTE flattens due to more cells coming into contact. Different load levels will also change the contact positions and number of teeth in mesh. The Fourier coefficients of the LTE are shown in Figures 3(b-c) for two loading conditions. Under light load, the LTE is dominated by the first harmonic. On the other hand, higher order mesh harmonics are seen to be more significant under heavier load. Also, the mean mesh stiffness is load dependent, and is a function of contact position, load and tooth profile modification.

Next, the free vibration of the corresponding linear model with time-invariant mesh stiffness and force vector is analyzed. A typical hypoid gear set given by Table 1 is used for this study. Three types of linear modes are identified: (i) out-of-phase gear rotation at the mesh coupled with translation motion of the pinion and/or gear; (ii) in-phase gear rotation at the mesh coupled with translation motion of pinion and/or gear; and (iii) pure translation motion of pinion and/or gear body. The predicted modes and their natural frequencies are provided in Table 2 for three input pinion torque levels. Modes 5 and 8 are pure translations that are decoupled from the mesh coupling coordinate. Thus, their corresponding natural frequencies are independent of load or mesh stiffness. On the other hand, the natural frequencies corresponding to the modes with strong gear mesh dependency such as modes 7 and 9 vary more with load. Note that the natural frequencies will also be affected by the change in mesh position and line-of-action, which in turn are load-dependent too.

To investigate the forced response for different loading cases, four load scales corresponding to 1000, 2000, 4500, 7000 in-lbf are used to study the effect of the mean torque applied to drive the pinion. The mesh force spectra for 3 different input torques are shown in Figures 4 using their respective mesh stiffness values. Under lightly loaded

conditions (1000 in-lbf), tooth separation occurs between 1250 Hz and 1830 Hz. This produces the classical jump phenomenon, where the frequency response is discontinuous in the vicinity of the resonant frequency. In this case, it is noted that the upper response branch is obtained from decreasing the rotational speed in the simulation, while the lower response branch is formed by increasing the rotating speed. This non-linear behavior is analogous to the phenomena of a softening spring. It may be noted that a higher TE under a lighter load does not show increase in response since the load also modify the mesh stiffness value. This change in mesh stiffness will in turn contribute to the amplitude of the forced response. Also, note that the tooth separation phenomenon is not observed for input loads 4500 and 7000 in-lbf because the teeth always maintain continuous contact and the system behaves much like a linear time-invariant system in spite of the backlash present. One of the reasons that separation occurs at light load rather than heavy case because the LTE is larger for lighter load compared to the other 2 higher torques. It is also interesting to note that the resonant frequencies shifted to lower values when input torque is reduced. This is due to the fact that the mesh stiffness is lower than that at high load, as pointed out previously.

To study the excitation of harmonics of LTE, two cases based on the linear dynamic model with constant mesh stiffness were simulated. The first case used a sinusoidal LTE (fundamental LTE), and the second problem used the first three harmonic spectra of LTE with constant mesh stiffness. The mesh force responses from these two cases are shown in Figure 5. It can be seen that the fundamental LTE excites only mode 7 (f_7=799.7 Hz), and the second harmonic of LTE seems to excite the mesh force resonance at f_m=890 Hz, which is $f_o/2$ or $2f_m$ type super-harmonics.

To investigate the load effect on the non-linear forced response, further simulations were performed under two relatively light loads. Figure 6 shows the frequency response functions of the dynamic transmission error for 1000 and 2000 in-lbs along with the corresponding linear time-invariant solutions. It is noted that the jump frequencies are dependent on the torque as the result of the load dependent mean mesh stiffness utilized. The primary resonant modes are 1, 3, 7 and 9, which are essentially the out-of-phase torsional motion coupled with translation motion of the gear pair. The resonance frequencies around 480 Hz for 1000 in-lbf and 580 Hz for 2000in-lbf are not the primary modes associated with free vibration problem. Rather, they are the super-harmonics generated by the higher harmonics of LTE. To justify this observation, the FFT spectrum of the response time trace at 2000 in-lbf is illustrated in Figure 7. It shows that even though the system is operated at f_m=580Hz. Hz, the response was clearly dominated in part by the $3f_m$ harmonic term, since the third order LTE harmonic appears to match mode 9.

SUMMARY

A new non-linear time-varying dynamic model of the hypoid gear pair, which includes the effect of coupled translation-torsion motion, is developed. In addition, the gear backlash and sliding friction effects are also incorporated into the theoretical model. The mesh characteristic is based on a 3-dimensional loaded tooth contact analysis for quasi-static condition. Modal property and forced response are computed, and calculation results show that the dominant modes are contained in the translation and torsion response. The occurrence of jump phenomenon is observed due to tooth separation/impact when the hypoid geared rotor system is subjected to low input torque. Also, the resonant vibration levels are determined to depend strongly on the loaded transmission error and mesh stiffness.

REFERENCES

1. Abe, E. and Hagiwara, H., 1990, "Advanced Method for Reduction in Axle Gear Noise," *Gear Design, Manufacturing and Inspection Manual*, Society of Automotive Engineers, Warrendale, PA, pp. 223-236.
2. Blankenship, G.W. and Singh, R., 1995, "Dynamic Force Transmissibility in Helical Gear Pairs," *Mech. Mach. Theory*, Vol. 30, pp. 323-339.
3. Cheng, Y. and Lim, T. C., 1998, "Dynamic Analysis of High Speed Hypoid Gears With Emphasis on Automotive Axle Noise Problem," *Proceedings, Power Transmission and Gearing Conference*, ASME, Atlanta, Georgia, DETC98/PTG-5784.
4. Donley, M. G., Lim, T.C. and Steyer, G.C., 1992, "Dynamic Analysis of Automotive Gearing Systems," *Journal of Passenger Cars*, Vol. 101, No. 6, pp. 77-87.
5. Fong, Z.H. and Tsay, C.B., 1991, "A Study on the Tooth Geometry and Cutting Machine Mechanisms of Spiral Bevel Gears," *Journal of Mechanical Design, Trans. ASME*, Vol. 113, pp.346-351.
6. Fong, Z.H. and Tsay, C.B., 1992, "Kinematical Optimization of Spiral Bevel Gears," *Journal of Mechanical Design, Trans. ASME*, Vol. 114, pp.498-506.
7. Gosselin, C., Cloutier, L. and Sankar, S., 1989, "Effects of the Machine Settings on the Transmission Error of Spiral Bevel Gears Cut by the Gleason Method," *Proc. 1989 Int. Power Transm*. Gearing Conf: New Technologies for Power Transmissions of the 90's. Chicago, IL. pp. 705-712.
8. Gosselin, C., Cloutier, L. and Nguyen, Q.D, 1995, "A General Formulation For the Calculation of The load Sharing and Transmission Error Under Load of Spiral Bevel and Hypoid Gears," *Mech. Mach. Theory*, Vol. 30, pp. 433-450.
9. Kahraman, A. and Singh R, 1990, "Non-linear Dynamics of a Spur Gear Pair," *Journal of Sound and Vibration*, Vol. 142, pp. 49-75.
10. Kiyono, S., Fujii, Y. and Suzuki, Y., 1981 "Analysis of Vibration of Bevel Gears," *Bulletins of JSME*, 24, 441-446.
11. Krenzer, T.J., 1981, "Tooth Contact Analysis of Spiral Bevel and Hypoid Gears Under Load," *SAE paper 810688*
12. Kubo, A., Tarutani, I., Gosselin, C., Nonaka, T., Aoyama, N. and Wang, Z., 1997, " Computer Based Approach for Evaluation of Operating Performances of Bevel and Hypoid Gears," *JSME International Journal Series III-Vibration Control Engineering for Industry*, Vol. 40, pp. 749-758.
13. Lim, T. and Cheng, Y., 1999, "A Theoretical Study of the Effect of Pinion Offset on the Dynamics of Hypoid Geared Rotor System," *Journal of Mechanical Design*, Vol. 121, pp. 594-601.
14. Lim, T.C. and Singh, R., 1990, "Vibration Transmission Through Rolling Element Bearings. Part I: Bearing Stiffness Formulation," *Journal of Sound and Vibration*, Vol. 139, pp. 179-199.
15. Litvin, F L., Wang, A G. and Handschuh, R F., 1998, "Computerized Generation and Simulation of Meshing and Contact of Spiral Bevel Gears with Improved Geometry,"

Computer Methods in Applied Mechanics & Engineering. Vol. 158 n 1-2 May 25, pp. 35-64.

16. Litvin, F. L. and Gutman,Y., 1981, "Method of Synthesis and Analysis for Hypoid Gear-drives of Format and Helixform," *Journal of Mechanical Design*, Vol. 103, pp. 83-113.
17. Litvin, F. L., 1989, *Theory of Gearing*, NASA Reference Publication 1212.Mark, W. D., 1987, "The Generalized Transmission Error of Spiral Bevel Gears," *Journal of Mechanisms, Transmissions, and Automation in Design*, Vol. 109, pp. 275-282.
18. Litvin, F. L. and Zhang, Y., 1991, "Local Synthesis and Tooth Contact Analysis of Face-milled Spiral Bevel Gear", *NASA Technical Report 4342* (AVSCOM 90-C-028), Washington, D.C.
19. Nakayashiki, A., et. al., 1983, "One Approach on the Axle Gear Noise Generated from the Torsional Vibration," *Proceedings - Society of Automotive Engineers* P-139. Vol. 2, Publ. by JSAE, Tokyo, Japan, pp. 571-580.
20. Özgüven , H. N. and Houser, D. R., 1988(a), "Mathematical Models Used in Gear Dynamic-A Review," *Journal of Sound and Vibration*, Vol. 121, pp. 383-411.
21. Özgüven , H. N. and Houser, D. R., 1988(b), "Dynamic Analysis of High Speed Gears By Using Loaded Static Transmission Error," *Journal of Sound and Vibration*, Vol. 125, pp. 71-83.
22. Pitts. L.S., 1972, "Bevel and Hypoid Gear noise Reduction," *SAE Paper* 720734.
23. Remmers, E. P., 1971, "Dynamics of Automotive Rear Axle Gear Noise," *SAE paper* 710114.
24. Tavakoli, M.S. and Houser, D.R., 1986, "Optimum Profile Modifications for the Minimization of Static Transmission Errors of Spur Gears," *J. of Mechanisms, Transmission and Automations in Design*, Vol. 108, pp. 86-94.
25. Velex, P and Maatar, M., 1996, "A Mathematical Model For Analyzing The Influence of Shape Deviations and Mounting Errors on Gear Dynamic Behavior," *J. Sound and Vibration*, Vol. 191(5), 629-660.
26. Vijayakar, S., 1987, "Finite Element Methods for Quasi-prismatic Bodies With Application To Gears," *Ph.D Dissertation*, The Ohio State University, Columbus, Ohio,USA.
27. Vijayakar, S., 1991, "A combined surface integral and finite element solution for a three-dimensional contact problem," *International Journal for Numerical Methods in Engineering*, vol. 31, pp. 525-545.

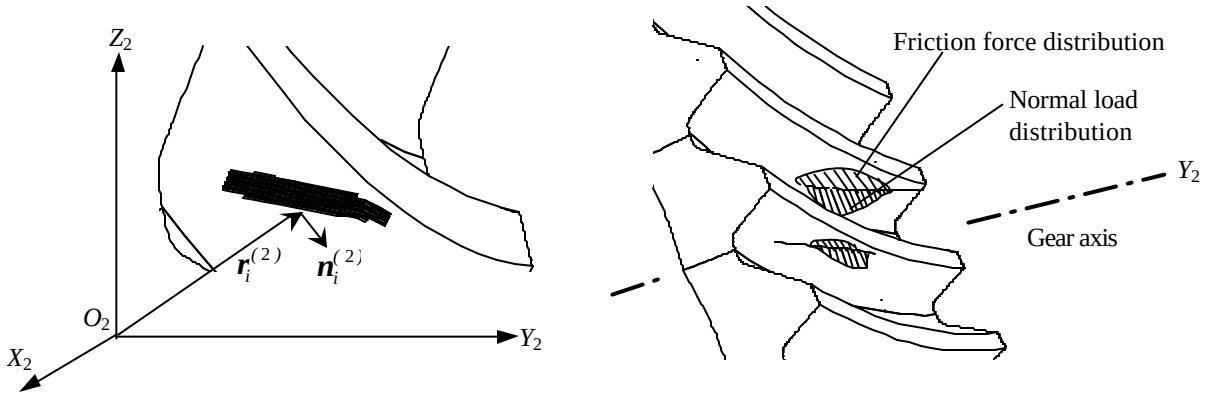

Figure 1. Contact cells and load distributions at the gear surface.

Table 1. Hypoid gear design parameters used in case study.

Number of teeth (pinion/gear)	10 / 43	Machine center to back (mm)	1.270
Face width (mm)	48	Horizontal setting (mm)	85.598
Pinion offset (mm)	31.75	Vertical setting (mm)	96.177
Mean cone distance (mm)	152.14	Cutter blade angle	0.3927
Ratio of roll	3.9936	Nominal radius (mm)	114.30
Blank offset (mm)	24.542	Point width (mm)	3.81
Machine root angle	-0.0226	Cutter blade angle	0.3491
Point radius (mm)	108.450	Machine center to back (mm)	-4.5847
Radial setting (mm)	118.513	Basic swivel angle	-0.7046
Equivalent inertia of pinion (kg-m^2)	0.1300	Basic cradle angel	1.0614
Inertia of engine unit (kg-m^2)	5.5E-3	Sliding base (mm)	18.242
Inertia of load unit (kg-m^2)	0.1	Equivalent inertia of gear (kg-m^2)	1.4188
Equivalent mass of pinion assembly (kg)	60.0	Torsional stiffness of pinion shaft (Nm/rad)	1.0E4
Equivalent mass of gear assembly (kg)	80.0	Torsional stiffness of gear shaft (Nm/rad)	5.0E5
Torsional support stiffness (Nm/rad)	2.0E8	Axial support stiffness (N/m)	1.5E7
Machine root angle	1.2287	Lateral support stiffness (N/m)	3.8E8

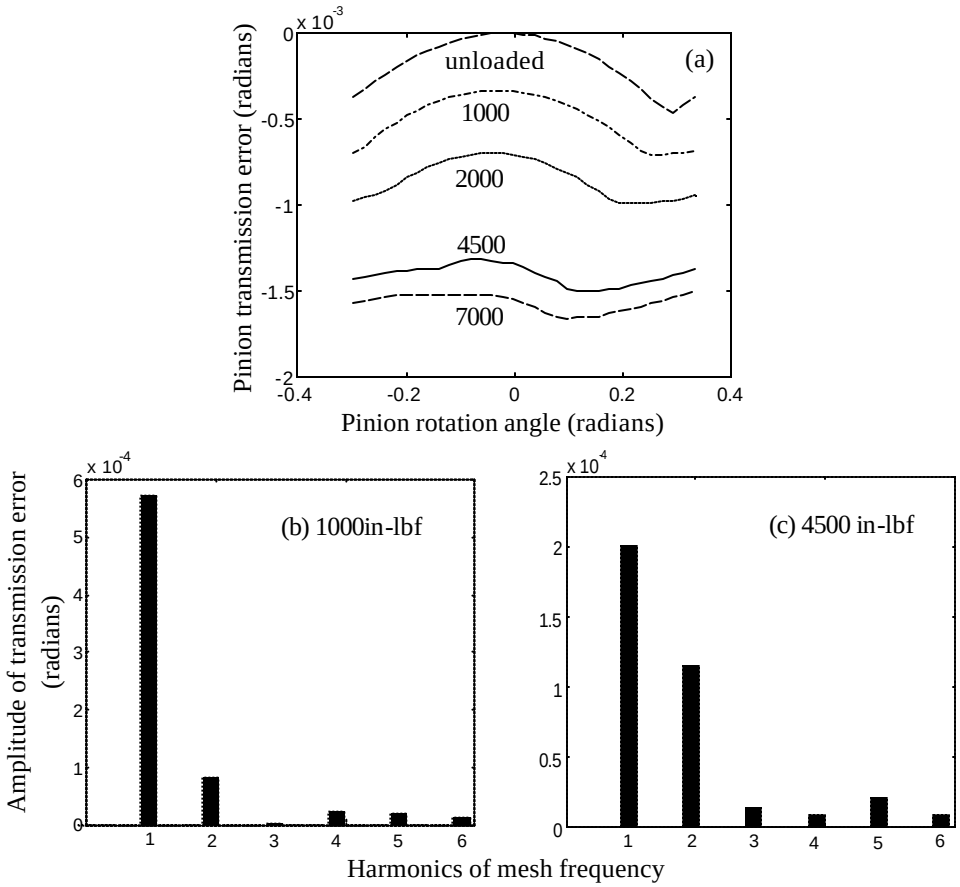

Figure 3. Loaded transmission error and Fourier coefficients of loaded transmission error under two different pinion torques.

Table 2. Classification of mode shapes.

Mode Type	Mode Description	Natural Frequency (Hz)		
		1000 in-lbf	2000 in-lbf	4500 in-lbf
In-phase torsion-translation	2 (Y_1, Y_2, q_E)	222.4	222.6	222.2
Pure translation	5 (Z_2)	427.4	427.4	427.4
	8 (X_1)	887.9	887.9	887.9
Out-of-phase torsion-translation	1 (Y_1, Y_2, q_E)	204.1	205.1	205.2
	3 $(Y_1, X_2, Z_2, q_E, q_O)$	342.7	344.2	344.4
	4 (Y_1, X_2, Z_2, q_O)	391.2	391.3	391.3
	6 (Y_1, X_2, Z_2, q_O)	436.6	436.6	436.5
	7 (Z_1, Y_1, X_2, Z_2)	786.0	797.0	799.7
	9 (Z_1, Y_1)	1450.0	1704.4	1799.1

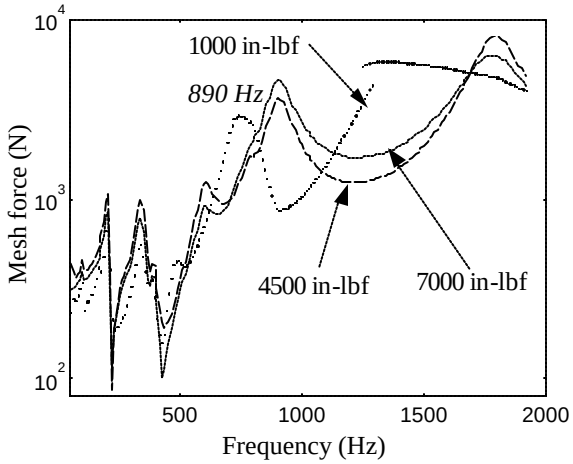

Figure 4. Dynamic mesh forces for 3 loads (no friction).

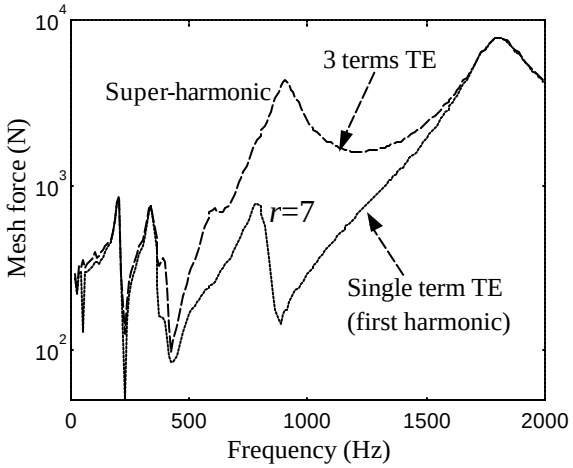

Figure 5. Dynamic mesh forces due to fundamental and first 3 harmonics of TE (4500 in-lbf, no friction, time-varying mesh vector and constant k_m).

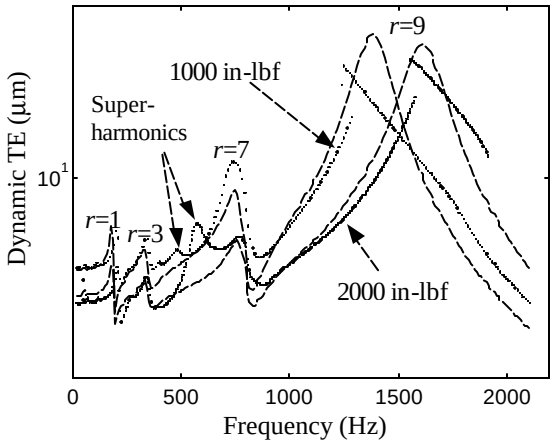

Figure 6. Dynamic transmission errors of non-linear and linear models (constant k_m, no friction).

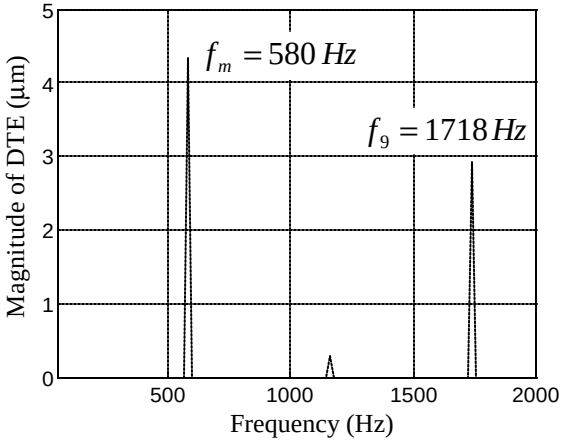

Figure 7. Spectrum of dynamic TE at operating frequency of 580Hz for 2000 in-lbf case.